International Journal of Innovation and Applied Studies
ISSN 2028-9324 Vol. 30 No. 2 Aug. 2020, pp. 642-659

http://www.ijias.issr-journals.org/

Interpretation of geophysical data and contribution to improving the knowledge of an oil and gas lead from the Congo Basin: Case of lead A in block 7 of the Cuvette Centrale basin in DR Congo

Eli-Achille Manwana Mfumukani[1-3], Joseph Pilipili Mawezi[2-3], Raïs Seki Lenzo[1-2-4], Lievens Masengo Mishindo[5], Hugues Makima Moyikula[2-4-6], Rally Kimpese Talong[2-4], Grady Kalonji Lelo[2], and Alidor Kazadi Mutambayi[1]

[1]Department of Internal Geophysics, Center of Research in Geophysics (CRG), Kinshasa, RD Congo

[2]Department of Exploration and Production, Faculty of Oil, Gas and New Energies, University of Kinshasa, Kinshasa, RD Congo

[3]Department of Geosciences, Mash Wait Company, Kinshasa, RD Congo

[4]Laboratory for Hydraulic Development and Energy Production Engineering (LAH-IPE), University of Kinshasa, Kinshasa, RD Congo

[5]Department of Physics and Applied Sciences, National Pedagogical University, Kinshasa, RD Congo

[6]National Center for Remote Sensing (CNT), Kinshasa, RD Congo

ABSTRACT: The purpose of the present work is to use gravity and magnetic data to improve the knowledge of the lead A of the petroleum block 7 of the Cuvette Centrale sedimentary basin in the DR Congo. These data were processed using the regional-residual separation method in order to make a detailed study of the basement and the thick sedimentary cover. As a result, we noticed that this lead rests on a basement uplift zone wedged between the sub-basins of Busira in the west and Lomami in the east. It is therefore an ideal location to receive the oil and gas expelled from these two depocenters. The horizontal derivative maps allowed us to identify the multiple faults that cut into the geological formations due to compressive events and the lifting of the dome-shaped basement at this location. Thanks to 3D modeling we found that the compression that caused this significant uplift of the basement generated several antiform folds and salt domes above this large dome. The Half-Width method was used to estimate the depth of certain identified sources. The integration of the R9 seismic profile in the interpretation of the data allowed us to have a much clearer picture on the important oil targets in this lead. At the end of this study we established a petroleum structural map of the region which improves our knowledge on the structures of petroleum interest having played a major role both in the process of migration of hydrocarbons and in their trapping.

KEYWORDS: geophysical data, knowledge, oil, gas, basin, Congo.

1 INTRODUCTION

The Cuvette Centrale sedimentary basin is an area with enormous mining and petroleum potential. Because of its oil potential in particular, this region has aroused the interest of many oil companies since the 1950s who have carried out multiple works based on geochemistry, geology, geophysics as well as the drilling of 5 wells. The results of all these studies suggest the existence of several petroleum systems in which hydrocarbons could have been generated (Mello, 2006 [1]). The structural model which was highlighted at the end of these studies made it possible to subdivide this basin into several sub-basins separated by structural highs. The seismic structural interpretation made in 1988 by Exploration Consultant Limited (ECL) [2] identified most of these structural highs as leads. In all case the highlighted areas of closure are extremely large but require a denser seismic grid for better definition. As part of this study, we will deepen our knowledge of lead A in block 7, which has an area of approximately 1,905 km² (fig. 1).

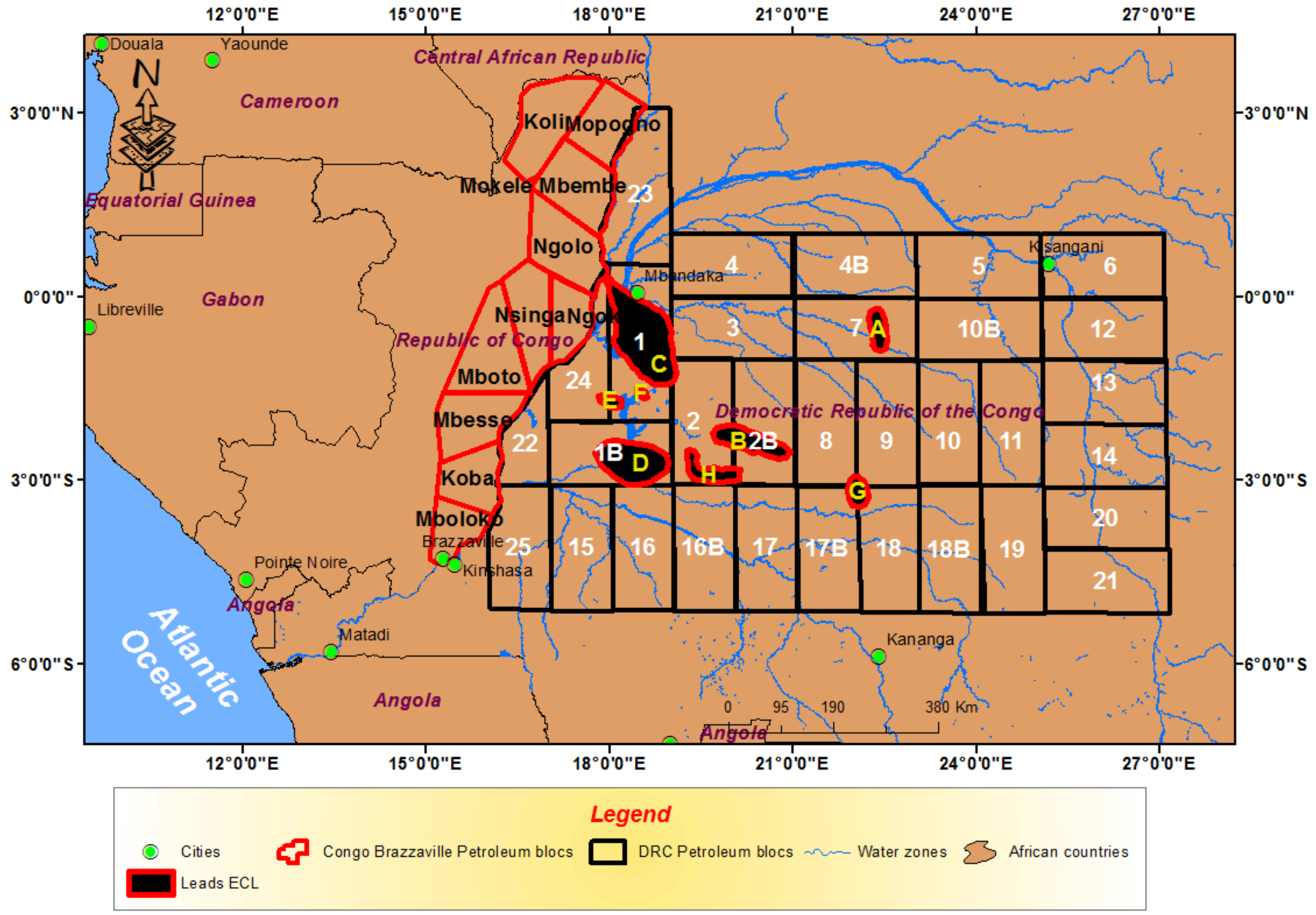

Fig. 1. Map of the location of the different leads of the Cuvette Centrale basin

2 MATERIAL AND METHOD

We used several data processing methods to achieve the final result. A reduction the pole (RTP) filter was previously applied to the magnetic data in order to eliminate distortions of anomalies. These were then mapped using the Minimum Curvature interpolation method. The Bouguer anomalies were mapped using Kriging as an interpolation method and separated into regional and residual anomalies in order to make a detailed study of the basement and the thick sedimentary cover. Then these gravity and magnetic data were transformed into horizontal derivative maps and modeled in 3D in order to better identify the structures. Tracing the profiles allowed us to use the Half-Width method to estimate the depth of the sources. Finally, all the results obtained were calibrated with the R9 seismic profile in order to have a clear image of the oil targets in this lead. Note also that several earth science modeling software such as Geosoft Oasis montaj, OriginPro, ArcGis and Golden Surfer allowed us to do this work.

3 General Overview Of The Study Area

3.1 Location

The Block 7 of the Cuvette Centrale basin is entirely located in the province of Tshuapa in DR Congo and it crosses the territories of Boende, Bokungu and Ikela. It is located between 21° and 23° east longitude and 0° and 1° south latitude. It has an area of approximately 25,000 km² (fig. 2).

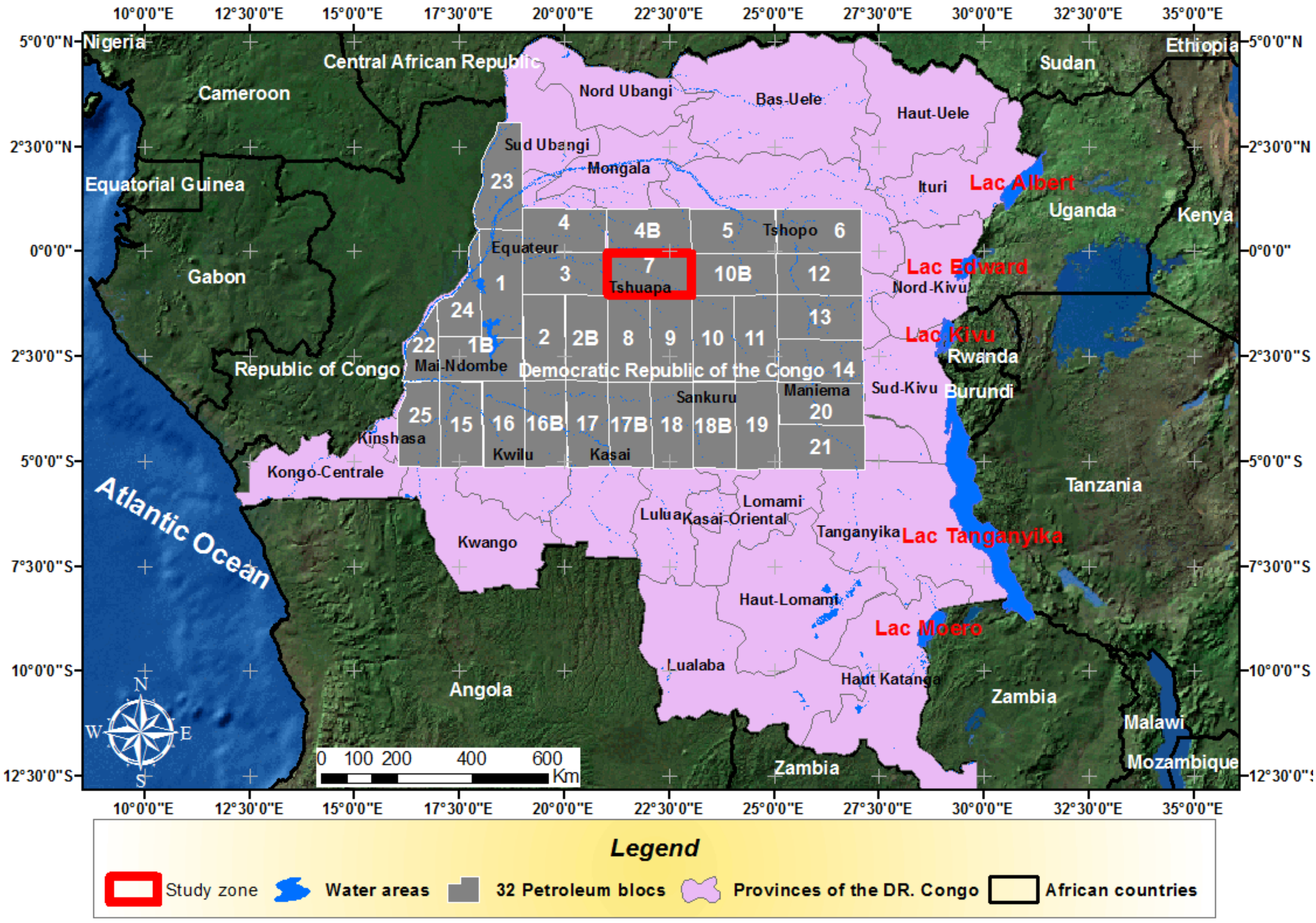

Fig. 2. Map of the location of block 7 of the Cuvette Centrale basin

3.2 Geography Of The Study Area

The area is characterized by the predominance of evergreen rainforest type rainforest landscapes. We also observe floodable and / or swampy forests along rivers and streams. The province of Tshuapa is classified in the zone "Af " in the classification of Koppen in which the dry season is almost non-existent because the climate which reigns there is of equatorial type with an average annual rainfall of the order of 2,000 mm. However, there is a marked decrease in rainfall in January and February. The wettest period is from August to October and the duration of the least rainy period (January-February) is less than 2 months (COMIFAC, 2005 [3]).

The relief of the area is characterized by marshy or floodable lowlands. Its altitude varies from 310 m in the west of the zone in the territory of Boende to 460 m in the territories of Ikela and Djolu in the east. The compilation of elevation data acquired during gravity and magnetic surveys carried out in this area allowed us to produce a Digital Terrain Model (fig. 3). Note also that the area has a large network of rivers, the most important of which are the Lomela and Tshuapa rivers.

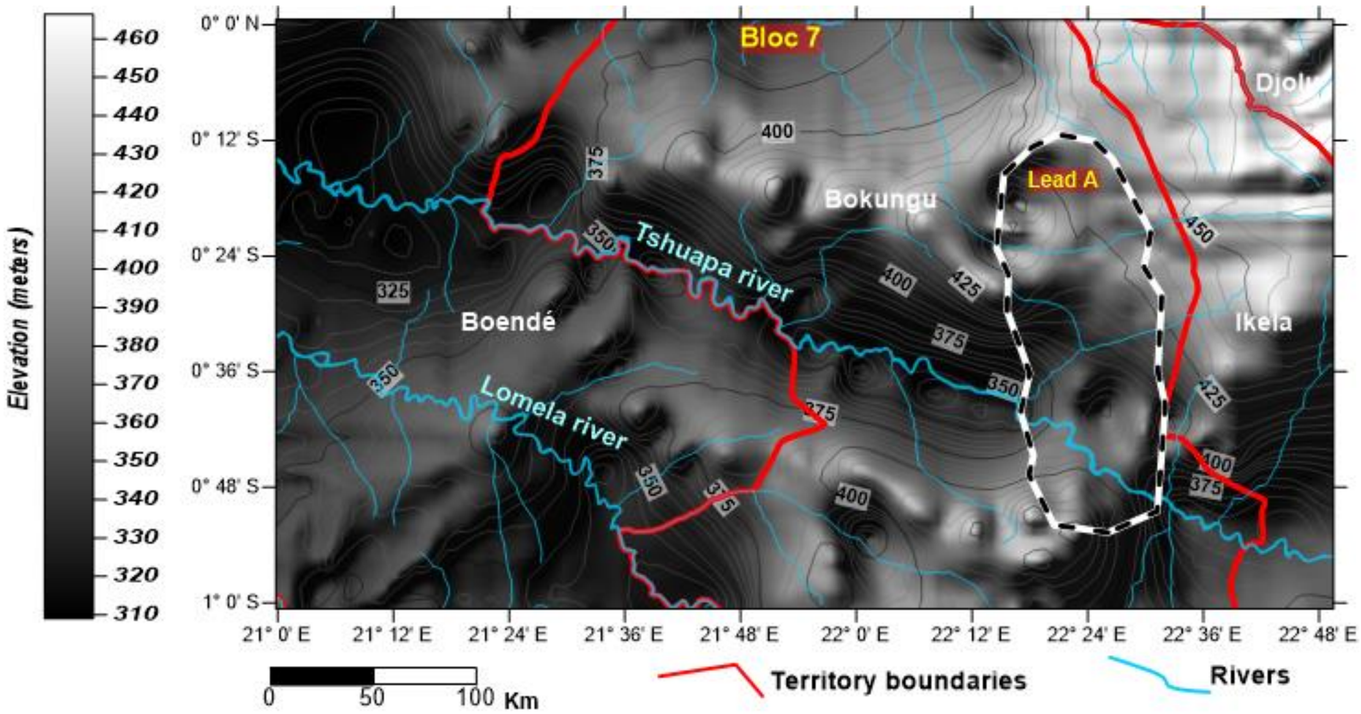

Fig. 3. Digital Terrain Model of the Block 7

3.3 GEOLOGY AND OIL INTEREST OF THE STUDY AREA

The area is mainly occupied by Cretaceous geological formations. The regional stratigraphy has been partially studied by the Samba-1 stratigraphic borehole (0°09'45"N; 21°15'10"E) located along the Maringa River in the northern part of the Tshuapa province. That borehole cuts through 1,167 m thick subhorizontal, red to green, bedded sandstones and mudstones, and then 871 m thick red quartzitic sandstones. The hole ends at a depth of 2,038 m, and does not reach the base of the quartzites (Bastien Linol and al 2015 [4]). As a result, the entire sequence from the lower Paleozoic to the Neoproterozoic was therefore not crossed by this well.

This drilling stopped at the base of the Upper Zaire Sequence (UZS) which is the equivalent of the "schisto-sandstone" series (Aruwimi group of the Middle Paleozoic) containing good reservoirs. More than 873 km thick in this borehole, this sequence contains two main play types. From top to bottom we have the Banalia red arkoses (Porosity: 13%; Permeability: 0.8 to 9.5 md) and the Galambonge sandstones (Porosity: 20%; Permeability: 14 md) (Unocal, 1987 [5]). These geological formations have the advantage of being based on thick horizons of source rocks: The Banalia arkoses rest on the Alolo black shales which have a Total Organic Carbon (TOC) of 3% while the Galambonge sandstones are trapped between the Alolo black shales which plays the role of cover rock on the top and the Kole and Mamungi formations (TOC: 5%) on the bottom. The Bobwamboli sandstones in the Lower Zaire Sequence (LZS) which is the equivalent of the Lokoma group of the Lower Paleozoic could also be an excellent reservoir.

The integration of all geological, geochemical and geophysical data available today suggested that the Congo Basin is an overcharged petroliferous basin that could be considered, today, one of the last province in Africa to hold giant to super-giant light oil, condensate and gas accumulations. The presence of oil seeps widespread around most of the Congo Basin suggests a light oil / gas prone system (Eni, 2011 [6]). The sizes of the structural highs considered as leads could be more than 1,000 km^2. Calculations based on lead A area provide a guide to the potential "In-place size" of oilfields which might be discovered. The in-place reserves were evaluated to 2.8 X 10^9 bbls (ECL, 1988 [2]).

4 Geophysical Data

4.1 Gravity Data

The gravity data used in this work were acquired by the "Société de Recherche Minière en Afrique" (REMINA) which collected around 6,550 stations in the Congo Basin between the years 1952 and 1956 (P. Evrard, 1957 [7]). These data were provided to us by the "Société Nationale des Hydrocarbures du Congo" (SONAHYDROC). They were then reduced using the classical Bouguer anomaly formula for a reduction density of 2.67 g/cm^3 in which a series of corrections is applied to the measurements in order to eliminate the non-geological causes of variations in the gravity, including topographic correction.

4.2 Magnetic Data

The magnetic datasets used for the study come from the African Magnetic Mapping Project (AMMP). The project, realized by Paterson, Grant & Watson Limited (PGW), in collaboration with GETECH and ITC, compiled all the available airborne and marine magnetic surveys (approximately 800) for the continent of Africa. These data have been acquired between 1948-1992 largely for hydrocarbon and mineral exploration interest. Focusing on the study area, several acquisition surveys have been performed by CGG service company in 1987. The flying height was approximately 1372 meters above the sea level.

Note also that the seismic profile of line R9 with a length of approximately 77 km oriented in the NW-SE direction acquired near the Tshuapa river was calibrated with gravity and magnetic profiles to have a better image of the main oil targets in this lead.

5 Interpretation Of Geophysical Data

5.1 Bouguer Anomaly Map

The Bouguer anomaly represents the attraction effect produced by the density of geological masses. It is the variations in density in the terrestrial globe which will create variations in gravity: below a heavy body gravity will be stronger than below a light body (J. Dubois and al., 2011 [8]). Gravity anomalies result from the difference in density, or density contrast, between a body of rock and its surroundings. For a body of density $\rho1$ embedded in material of density $\rho2$, the density contrast $\Delta\rho$ is given by the equation (1):

$$\Delta\rho = \rho1 - \rho2 \tag{1}$$

The sign of the density contrast determines the sign of the gravity anomaly (Philip Kearey, 2002 [9]).

On the Bouguer anomaly map below (fig. 4), the scale of values indicates that all of the Bouguer anomalies values are negative. It is justified by the fact that several kilometers thick of sedimentary rocks having an average density of 2.37 g/cm^3 rest on a Precambrian crystalline basement having an average density of 2.73 g/cm^3. The sediment / basement density contrast of is therefore, in our case, negative.

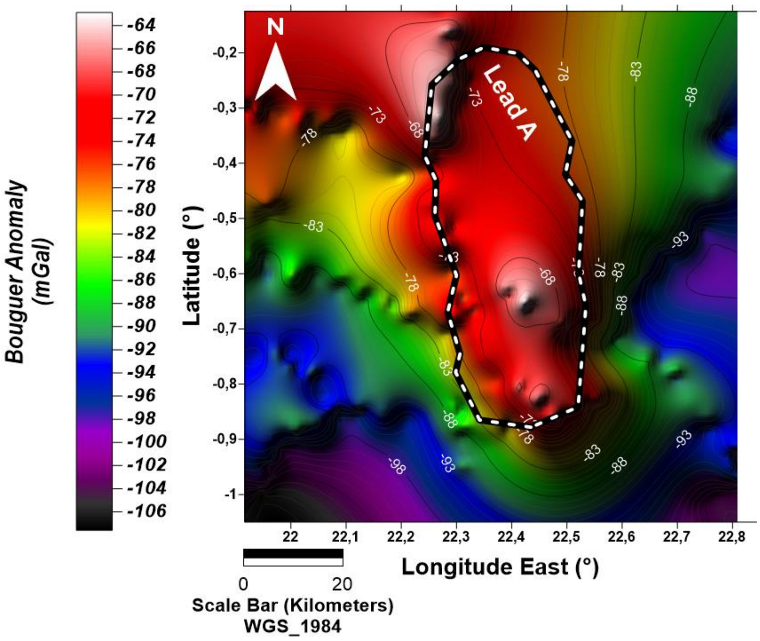

Fig. 4. Bouguer Anomaly Map of lead A

The map above allows us to better understand the structural configuration of our study area. High anomalies intensities (-78 to -64 mGals) cover the entire central part of the area, thus revealing the presence of high density materials. A very dense and shallow igneous and metamorphic basement would be at the base of this gravity high. By moving away from either side of this structure, the anomalies gradually decrease to reach values lower than -106 mGals to the east and the west of the zone indicating the presence of a subsided basement filled correlatively by a substantial sedimentary thickness.

5.2 GRAVITY REGIONAL ANOMALIES MAP

The spatial distribution of regional anomalies (fig. 5) is identical to that of the Bouguer anomaly map.

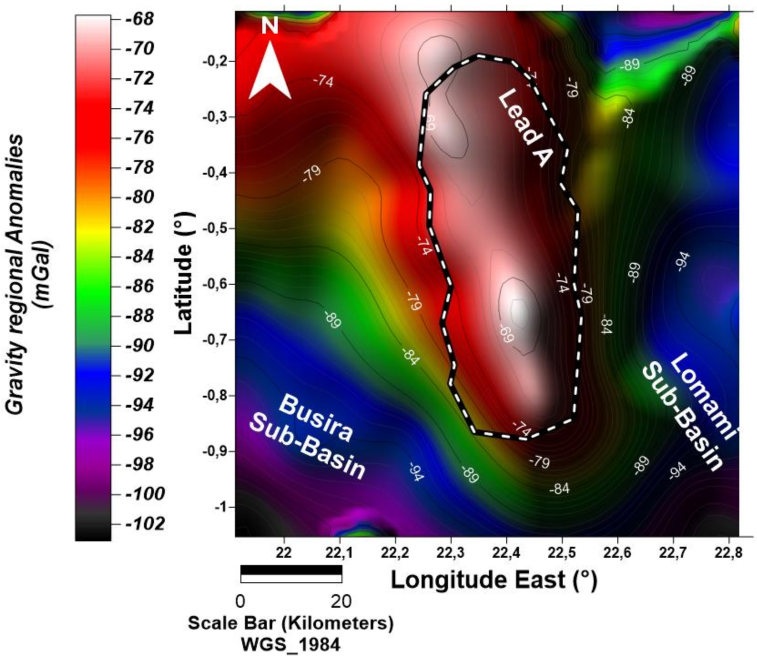

Fig. 5. Gravity regional anomalies map of lead A

The gravity high surrounded by significant negative anomalies is clearly identifiable on this map. It is a large horst of N-S orientation wedged between two depressions which are the sub-basins of Busira in the west and Lomami in the east. The demarcation between the horst and the depressions is so clear that it reveals the presence of major faults. Being a structural high bounded on both sides by vast depocenters, the lead A is ideally placed to receive the hydrocarbons expelled from these depocenters. It should also be noted that the compression and basement uplift at this location certainly favored the generation of vast antiform folds in the sedimentary column which are very interesting targets in petroleum exploration.

Profile A below drawn perpendicular to the horst direction gives us several information on the extension of this horst and the contrast of anomalies which it induces (fig.6).

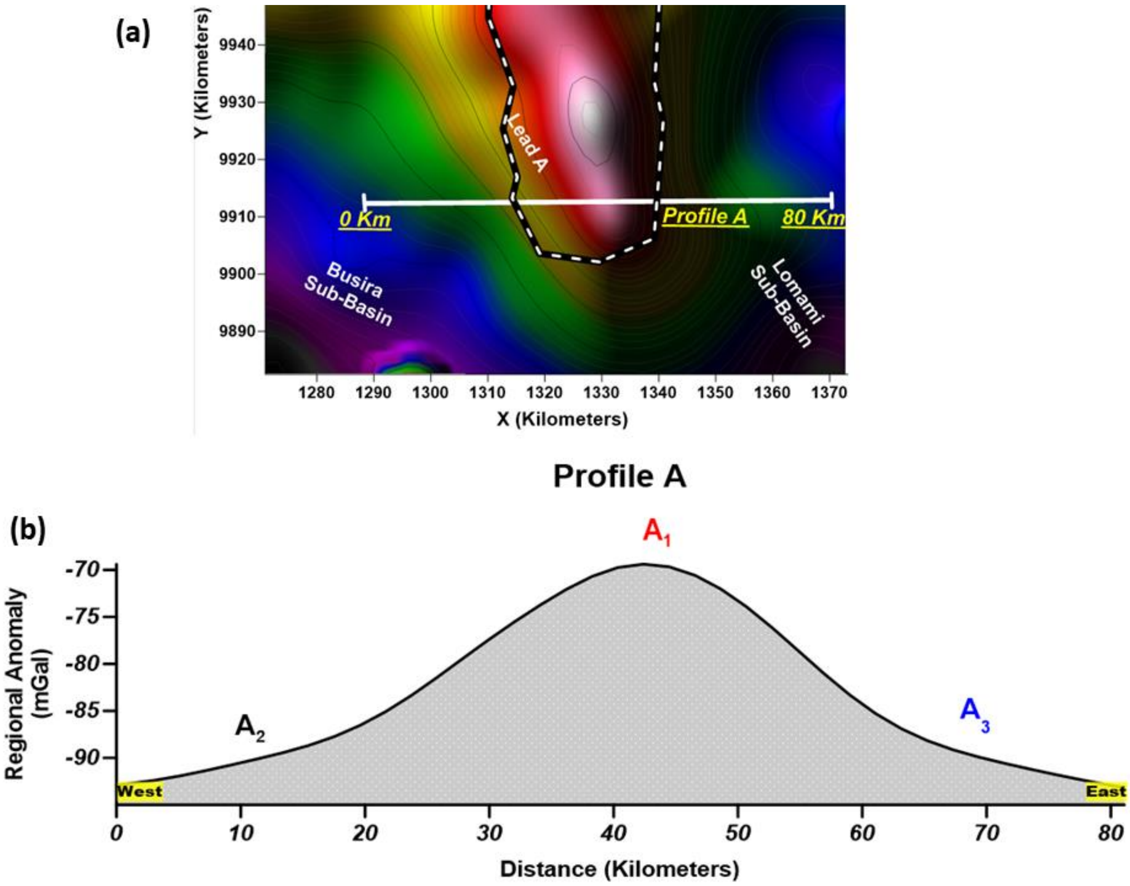

Fig. 6. (a) Location of profile A on the gravity regional anomalies map; (b) Profile A

This profile drawn in the southern part of the lead over a length of about 80 km perfectly illustrates the structure of this area. High intensities of anomalies (Δg max = -70 mGals) are observed in the center of the profile (Anomaly A1), indicating the presence of a horst. On both sides of this structure, we observe strong gravity depressions (Anomaly A2 and Anomaly A3) with values reaching -95 mGals. Such depressions indicate the gravimetric signatures of the collapse ditches. We also note that this uplift is very limited by very large contrasts of intensity, thus revealing the gravimetric signature of the faults.

5.3 Gravity Residual Anomalies Map

After the attenuation of the regional field, we notice the appearance of residual anomalies of small extension and short wavelengths. The residual anomalies map shows us small local disturbances in the gravitational field which are secondary in dimension but essential in the study of shallow geological structures (fig. 7).

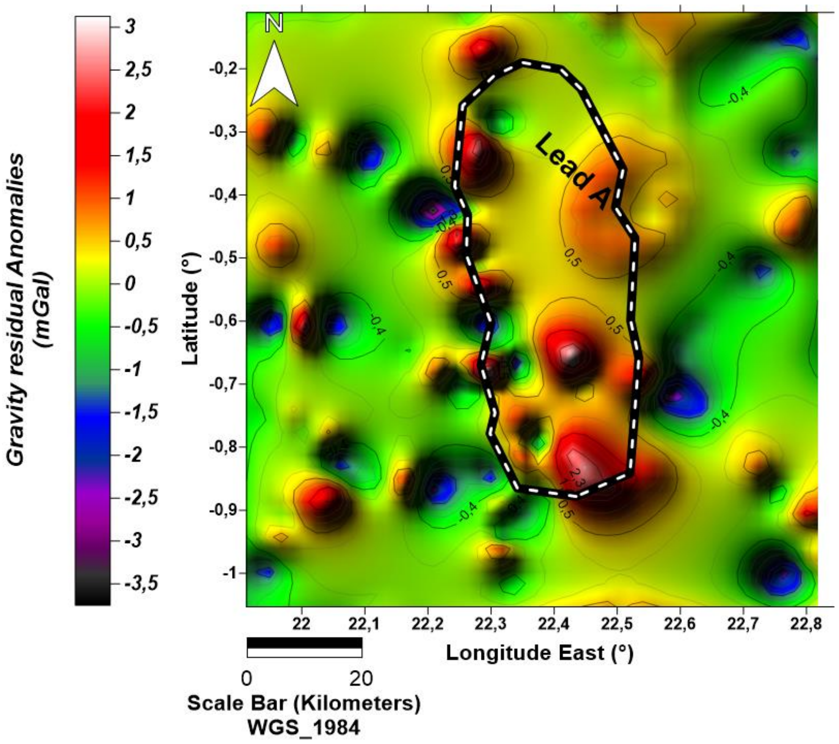

Fig. 7. Gravity residual anomalies map of lead A

The amplitude and characteristics of the gravity anomaly depend on the depth, the degree of sedimentary deformation and the integration of the basement in the studied geometry (Maroua ELFESSI, 1996 [10]). The sources generating residual anomalies in a sedimentary basin are generally the geological structures located in the sedimentary cover (salt domes, faults, folds, etc.). The quasi-circular shape and the intensity of these anomalies tell us about the type of structures present in this area:

- Positive anomalies indicate the presence of antiform folds affecting the sedimentary cover. Indeed, an anticline produces a positive and symmetrical gravity anomaly. This is how we observe several positive residual anomalies on the lead A which would be antiform structures generated by the compression and the basement uplift at this place. Note also that a magmatic intrusion in the sedimentary column could generate similar positive anomalies.
- Negative anomalies indicate the presence of synform folds or salt domes. Indeed, several studies have attested the presence of a salt tectonic in the structural evolution of the Congo Basin. Since salt is a lighter substance than the surrounding rocks, there will be a negative density contrast which will have the effect of locally reducing the intensity of the anomalies. This is how we generally observe negative gravity anomalies over the salt domes.

Profile B below has been drawn along the seismic line R9. Going from NW to SE, over a length of about 74 km, this gravity profile revealed four main anomalies in circular form which we name B1, B2, B3 and B4 (fig.8).

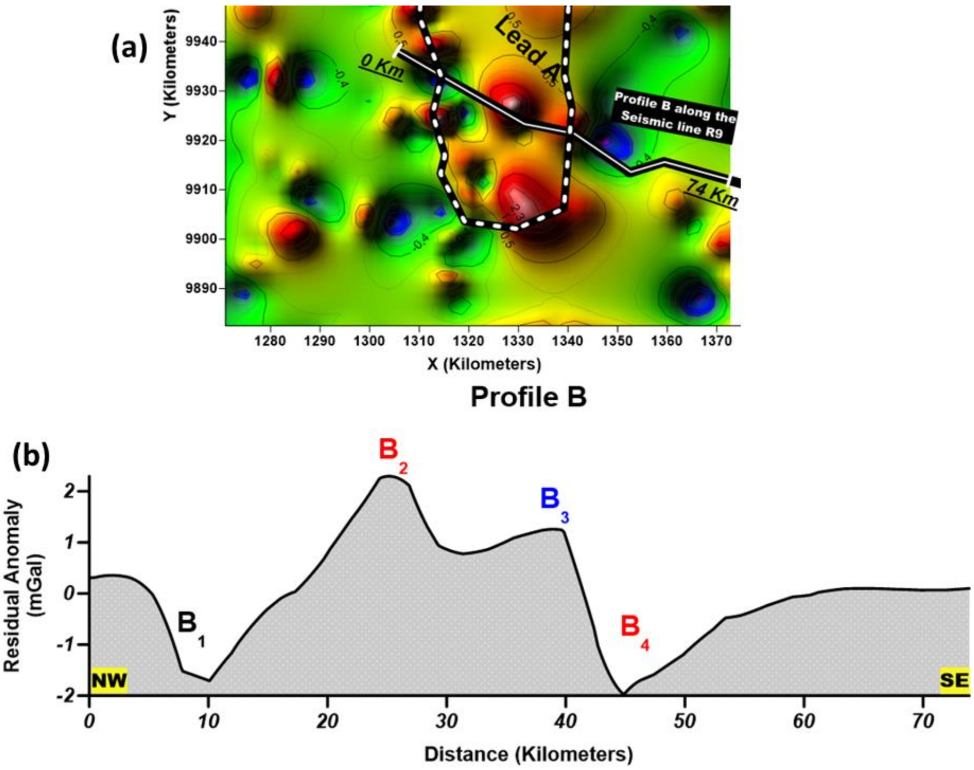

Fig. 8. (a) Location of profile B on the gravity residual anomalies map; (b) Profile B

The anomalies B1 and B4 are circular and negative, thus revealing the presence of an uplift of a low density substance. The salt dome hypothesis would be the most plausible in these two places. The B2 and B3 anomalies are also circular but positive in turn. The presence of a magmatic intrusion would produce similar anomalies, however the hypothesis of antiform folds in the sedimentary column would be the most plausible at these two locations. Indeed, these two anomalies are superimposed on the large regional anomalies A1 which corresponds to a significant basement uplift, as previously mentioned, would generate antiform folds. Note also that the uplift followed by the folding of the very dense schisto-limestone (Upper Neoproterozoic - Lower Paleozoic) series could increase the values of the anomaly.

5.4 GRAVITY HORIZONTAL DERIVATIVE MAPS

The horizontal derivative filters along the X and Y directions made it possible to determine the lateral density contrast zones which we separated into positive and negative axes according to the value of their intensity (fig. 9).

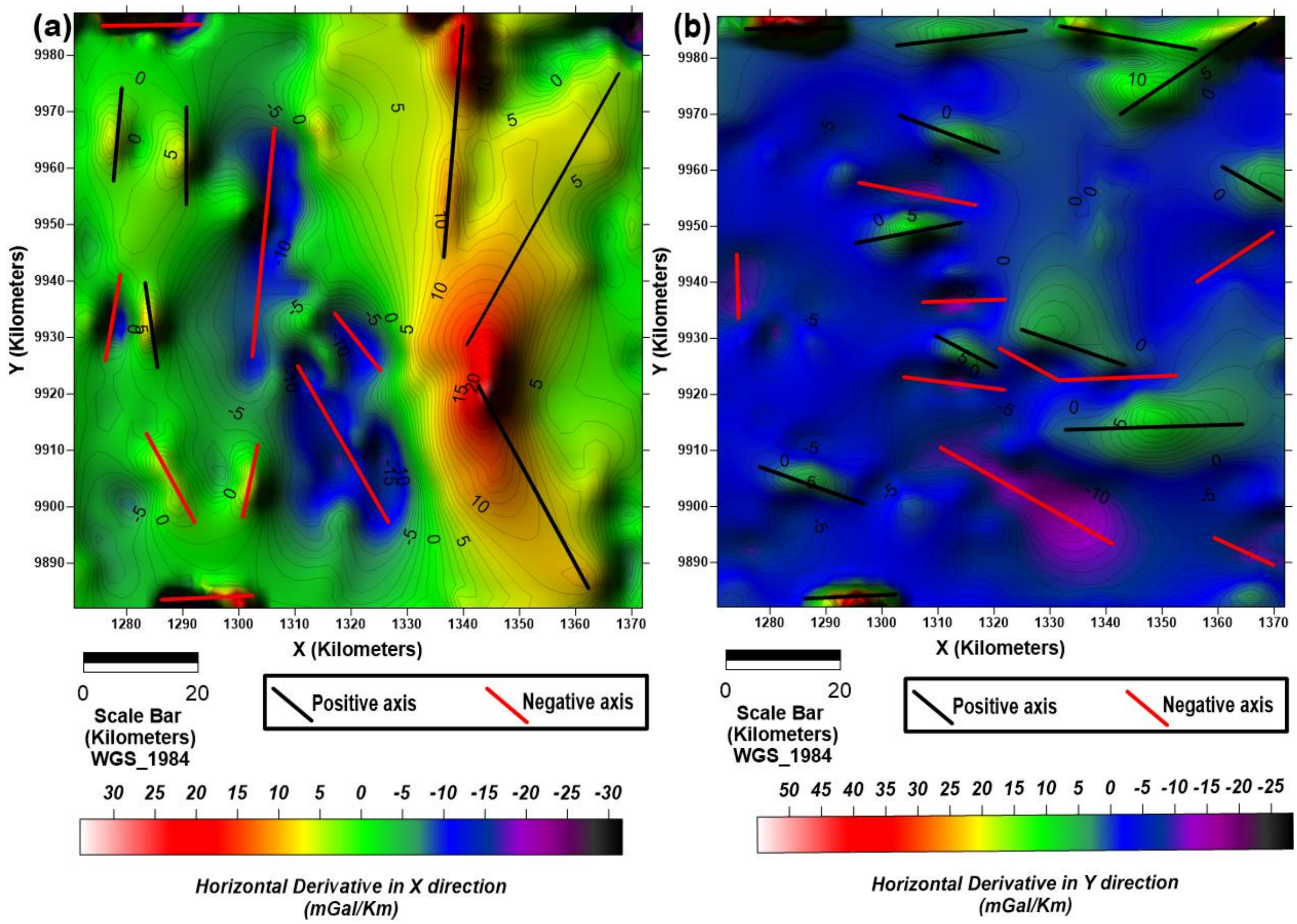

Fig. 9. Gravity horizontal derivative maps: (a) in X direction; (b) in Y direction

These axes are lineaments revealing the presence of several major tectonic accidents such as faults or lateral geological contacts. Note that the application of the horizontal derivative along the X axis has allowed us to locate the major lineaments parallel to the direction of the large horst, while the horizontal derivative along the Y axis has highlighted the lineaments oriented perpendicular to this one and secondary in dimension.

5.5 MAGNETIC ANOMALY MAP

The magnetic anomaly map has been reduced to the pole (RTP) in order to reposition the magnetic anomalies above the sources that caused them. To do this, we used the IGRF (International Geomagnetic Reference Field) geomagnetic model from 1985. This magnetic anomaly map RTP shows us very few lateral variations in intensity of anomalies because the high intensities (reddish color) cover approximately the ¾ of the map. Nevertheless, we note some average anomalies of quasi-circular shapes in the north and in the center, as well as important negative anomalies in the southeast of the map (fig. 10).

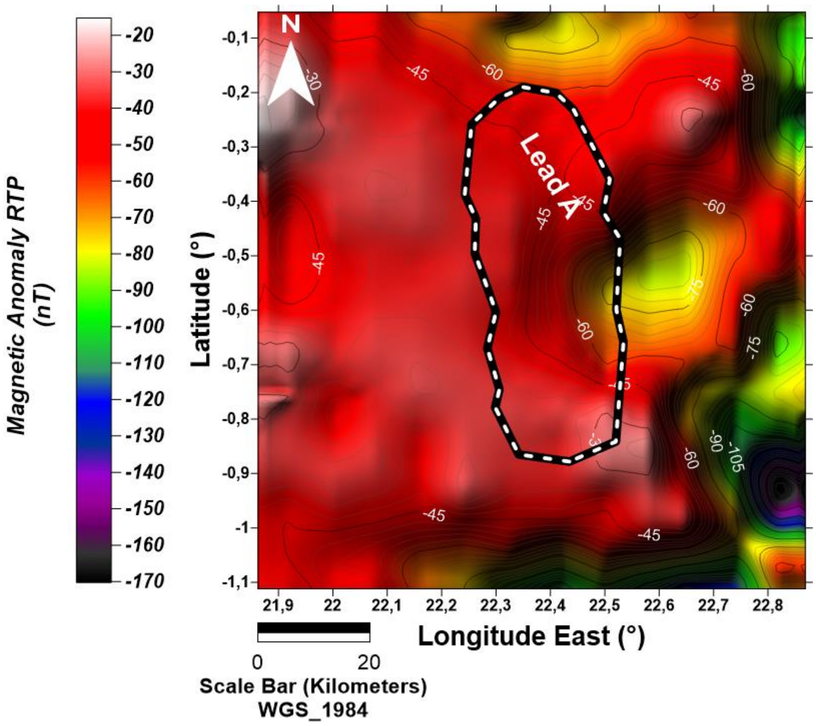

Fig. 10. Magnetic anomaly map RTP

We saw that the fundamental parameter in the gravity modeling was the density. In geomagnetism, it is the magnetic susceptibility of rocks which plays a similar role. It allows to characterize the composition of the rocks. Table 1 below gives some values of the magnetic susceptibility of rocks.

Table 1. Magnetic susceptibility of rocks (Michel Chouteau, 2002 [11])

Rock type	Average magnetic susceptibility x 10^{-4}
Basic igneous rocks	2600
Acid igneous rocks	650
Metamorphic rocks	350
Sedimentary rocks	75

We therefore find that igneous and metamorphic rocks have a very high magnetic susceptibility compared to sedimentary rocks. The magnetic anomaly map RTP tells us about the structure and composition of the rocks in this area. The high intensities reveal the presence of a regional uplift of the igneous and metamorphic rocks of the crystalline basement and the low intensity values in the southeast are correlated with the low intensities of gravity regional anomalies in the same place. They are certainly due to the subsidence of the basement and the thick sedimentary cover of very weak magnetic susceptibility. On the lead we observe high intensities of magnetic anomalies that can be correlated to high intensities of gravity regional anomalies which shows a significant basement uplift at this location accompanied by a probable mafic intrusion.

Like profile B, profile C below was also drawn by crossing lead A along the R9 seismic line over a length of approximately 74 km. Three large magnetic anomalies were detected (fig.11).

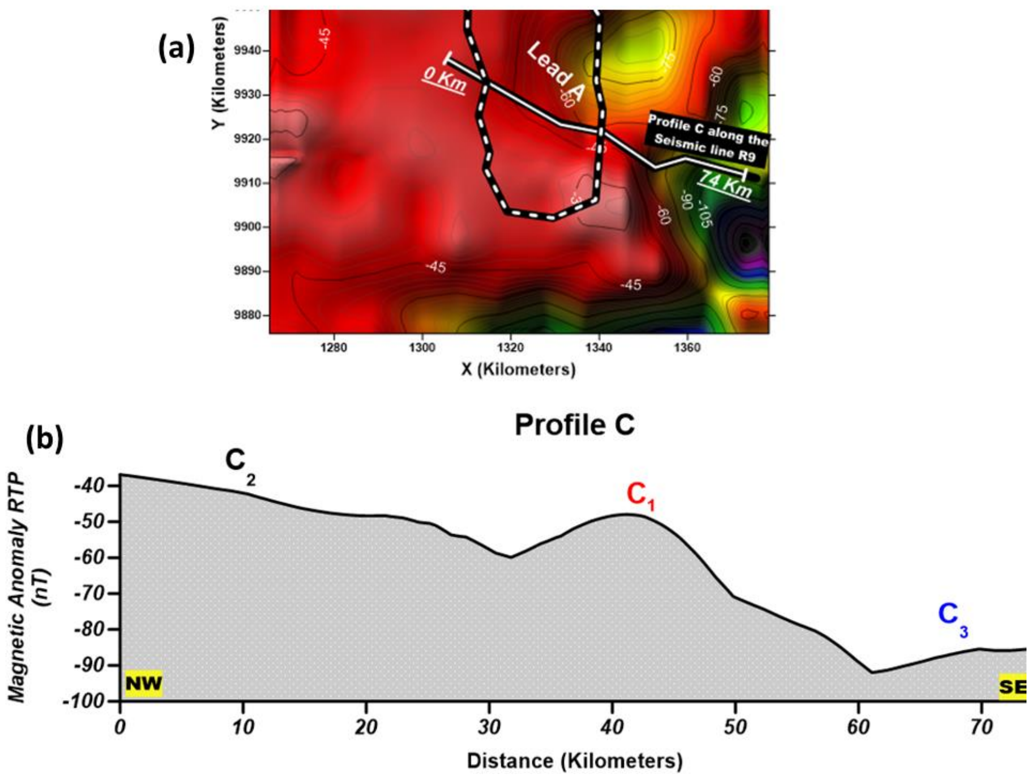

Fig. 11. (a) Location of profile C on the magnetic anomaly map RTP; (b) Profile C

The anomaly C1 corresponds to a mafic intrusion into the crystalline basement. This anomaly is separated from C2 by a slight depression in the basement about 32 km from the profile. The C2 anomaly also shows high intensities in the Northwest part, thus revealing the predominance of probably volcanic igneous rocks of very high magnetic susceptibility in the basement. Indeed, the more basic a rock, the higher its magnetite content (and therefore its susceptibility). For example, gabbros and ultrabasic rocks are generally more magnetic than a granite. Anomaly C3 corresponds to the Lomami sub-basin because the sedimentary material of low magnetic susceptibility is very thick in the area.

5.6 Horizontal Derivatives Maps Of The Magnetic Anomalies RTP

The horizontal derivative filters of the magnetic anomalies RTP along the X and Y directions revealed a very large number of lineaments in this area. These lineaments were also separated into positive and negative axes based on their intensity (fig. 12).

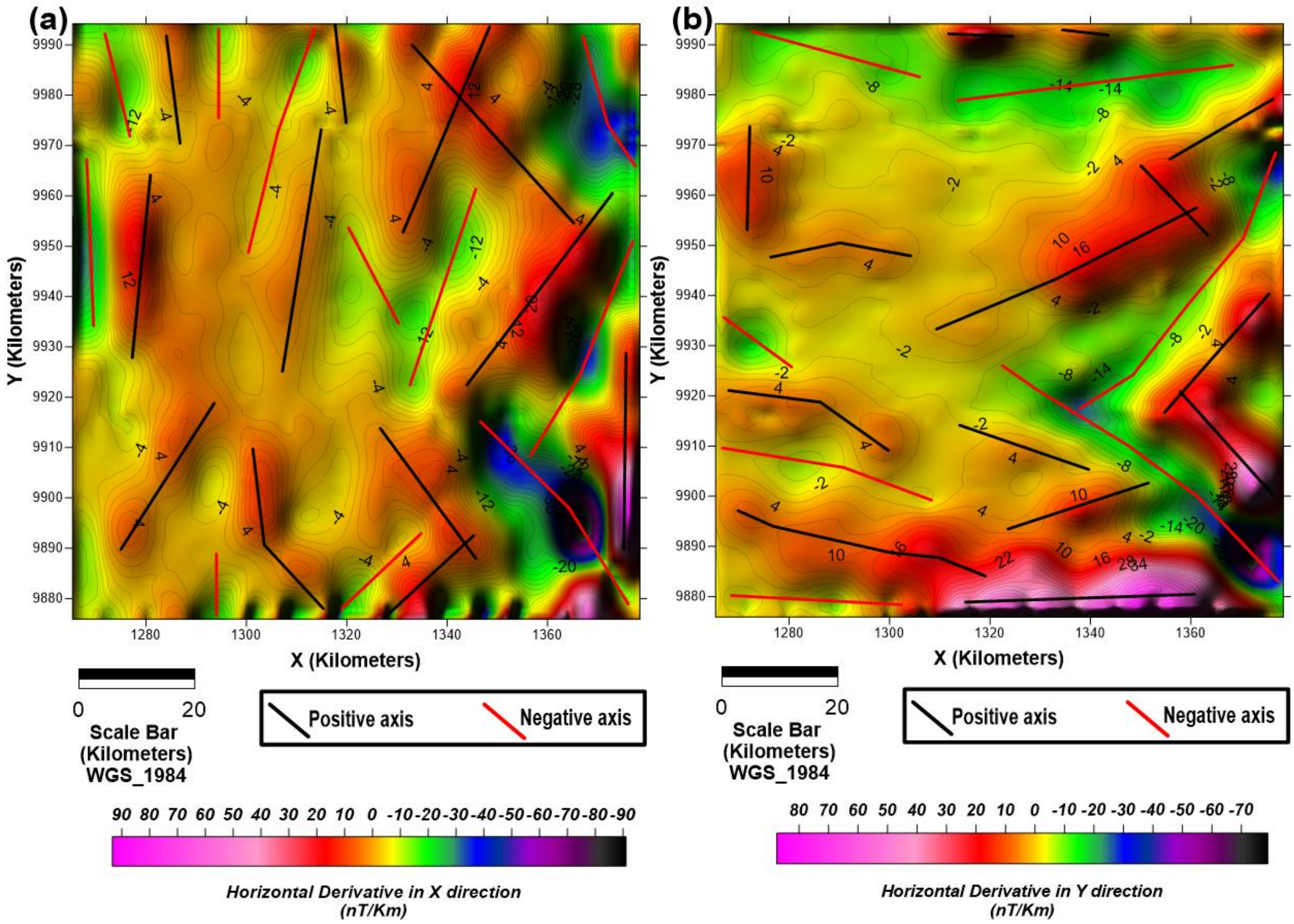

Fig. 12. Horizontal derivatives maps of the magnetic anomalies RTP: (a) in X direction; (b) in Y direction

We note that these tectonic accidents appear to be more numerous and, in general, more widespread than those identified by the gravity horizontal derivative maps. Since magnetic anomalies are essentially linked to the basement, these structures therefore reveal significant tectonic activity which affected the basement. However, the majority of the structural highs in the Congo Basin were formed and reactivated respectively by the Pan-African (Neoproterozoic-Paleozoic) and Hercynian (Permo-Triassic) compressive events. This is how we think that in addition to the basement, most of these faults also affected the sedimentary sequence from the Neoproterozoic to the lower Mesozoic. Recent sedimentary sequence would be less disrupted.

5.7 Depth Estimation Of Sources By The Half-Width Method

This method uses the projection of a certain point on the anomaly curve to have a direct estimate of the depth (Bouyahiaoui Boualem, 2010 [12]). Gravity and magnetic anomalies decay with the inverse square of the distance from their source so that anomalies caused by deep structures are of lower amplitude and greater extent than those caused by shallow sources. This wavenumber–amplitude relationship to depth may be quantified to compute the maximum depth (or limiting depth) at which the top of the anomalous body could be situated.

Using the simple model of an infinite vertical cylinder, the calculation of the depth of circular gravity and magnetic anomalies crossed by our different profiles is obtained by the following formulas:

For a magnetic anomaly:

$$h = 1{,}3\ x_{1/2} \tag{2}$$

In the case of a gravity anomaly, this formula becomes:

$$h = x_{1/2} \tag{3}$$

Where $x_{1/2}$ is the half-width of the anomaly at half-amplitude and *h* the maximum depth of the body.

Note that in the latter case, this method gives very high depths because gravimetry gives above all the depth of the center of the mass of a body than that of its top. Hence for a gravity anomaly, the depth of the top of a body is much less than the depth of its center. We then note:

$$h < x_{1/2} \tag{4}$$

Figure 13 below illustrates the different depth values calculated for the gravity and magnetic anomalies detected on profiles B and C. As the anomaly C3 is not completely crossed by profile C, its complex shape on this profile did not allow to estimate its depth. This is how we drew a new N-S profile completely crossing this circular magnetic anomaly to estimate its depth.

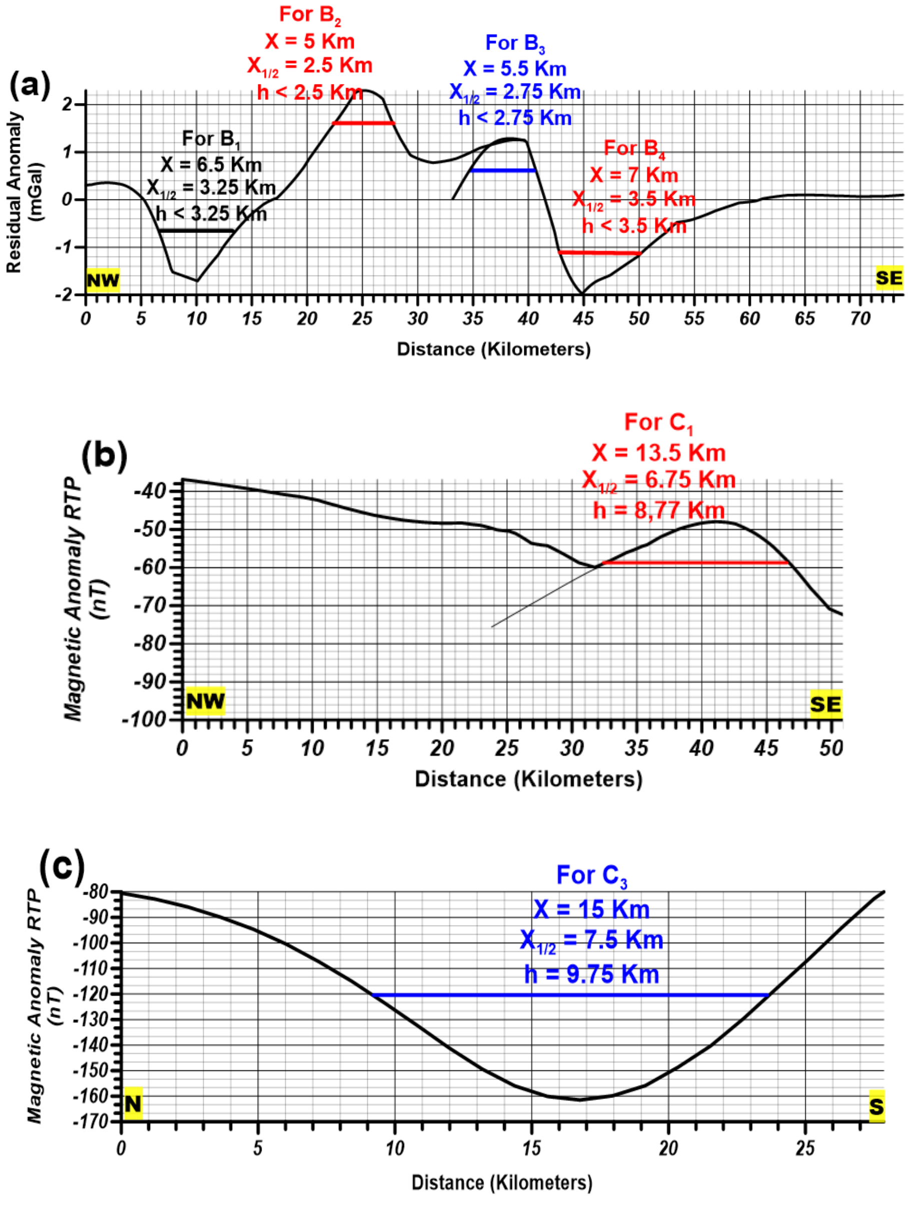

Fig. 13. Estimation of the sources depth on profiles B and C by the Half-Width method

The table 2 below summarizes all the depth values obtained for anomalies B1, B2, B3, B4, C1 and C2.

Table 2. Depths of sources

Anomalies	B1	B2	B3	B4	C1	C2
$X_{1/2}$ (km)	3.25	2.5	2.75	3.5	6.75	7.5
Depth (km)	h < 3.25	h < 2.5	h < 2.75	h < 3.5	h = 8.77	h = 9.75

The large amplitude and short wavelength gravity anomalies crossed by profile B have enabled us to identify structures with depths of the order of 2.5 to 3.5 km. Each of these structures, that are the salt domes for B1 and B4 as well as antiform folds for B2 and B3, could constitute targets of major interest for the exploration of hydrocarbons. The very high depths obtained for the magnetic anomalies C1 and C2, indicate to us that these anomalies of long wavelengths come from the crystalline basement.

5.7.1 3D Modeling Of Anomalies

One of the advantages of converting gravity and magnetic data into a three-dimensional model of the subsurface is that the very visual final product allows explorers to better see and understand the distribution of the density and magnetic susceptibility of geological formations. In the figure 14 below, a 3D model has been generated by integrating the regional and residual gravity anomalies as well as the magnetic anomalies RTP.

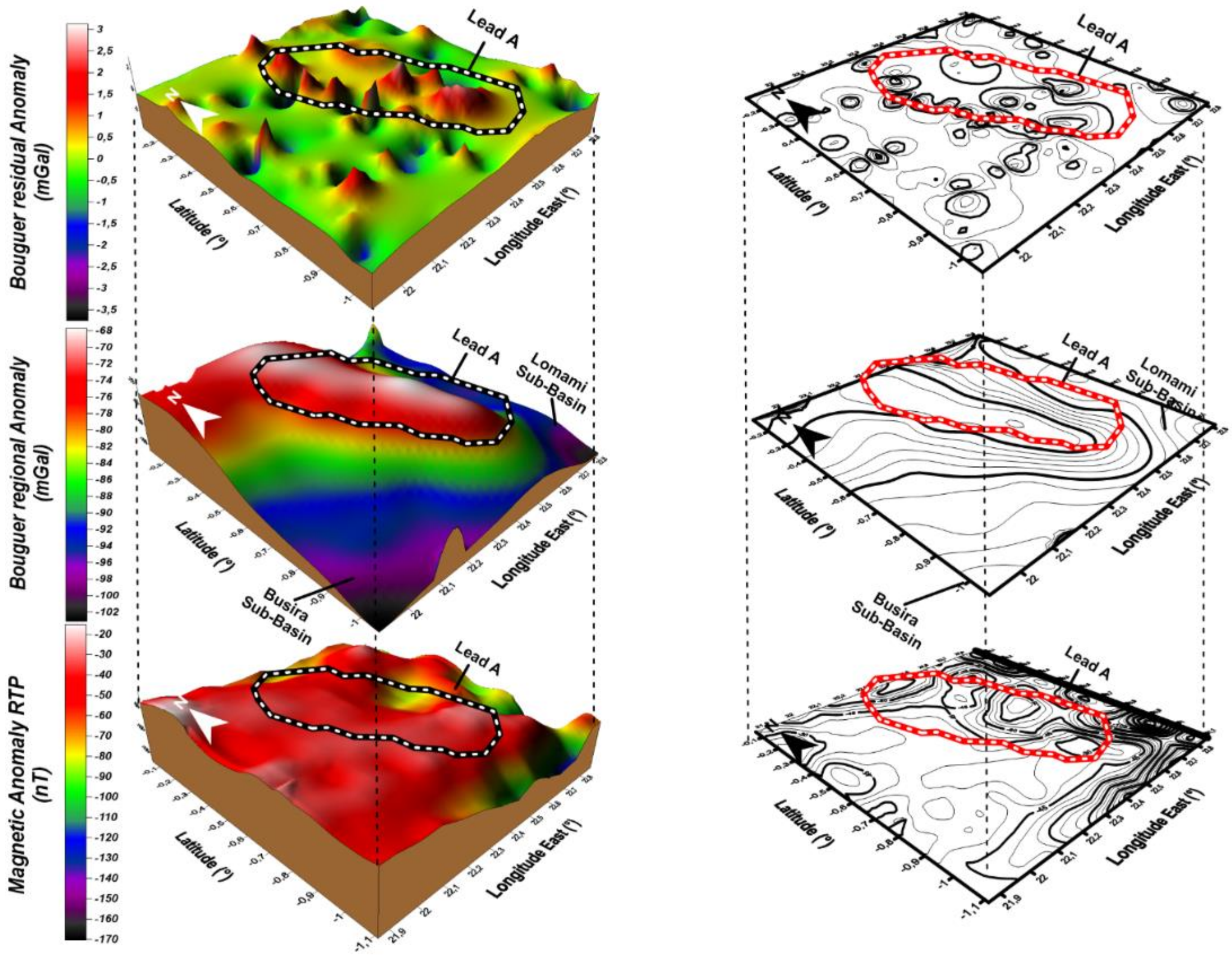

Fig. 14. 3D model of the anomalies

This model allows us to:

- Visualize the topography of the crystalline basement and get a first idea of its composition using the analysis of variations in gravity regional anomalies and magnetic anomalies;
- Have a much clearer overview of the various petroleum targets that could be the subject of much more exploration such as seismic and / or exploration drilling.

The very high magnetic anomalies on the lead correlate perfectly with the high intensities of gravity regional anomalies. We therefore confirm the hypothesis of a basement uplift accompanied by a possible mafic intrusion. Indeed, for igneous rocks, the density and magnetic susceptibility generally increase as a function of basicity. This is how basic and ultrabasic rocks are generally denser and more magnetic than acidic rocks. The presence of an uplift of mafic rocks in the basement at this location therefore generates significant gravity and magnetic anomalies.

Through this model we also confirm that the positive residual anomalies in the form of circular bulging revealing the presence of antiform structures in the sedimentary cover are strongly linked to the basement uplift due to compressive events. We have also noticed, on the different derivative maps, that these tectonics also generated several reverse and listric faults in this region. This lead is therefore a vast anticlinorium which could contain hydrocarbons in multiple places.

6 Results And Discussions

This geophysical study gave us several information which was enriched by the analysis of the R9 seismic profile and the stratigraphic log of the Samba-1 borehole for a better knowledge of the targets of major oil interest in our study area. The interpretation of gravity and magnetic anomaly maps allowed us to draw up a petroleum structural map of the region which improves our knowledge of the structures of oil interest which played a major role both in the hydrocarbon migration process and in trapping them (fig. 15).

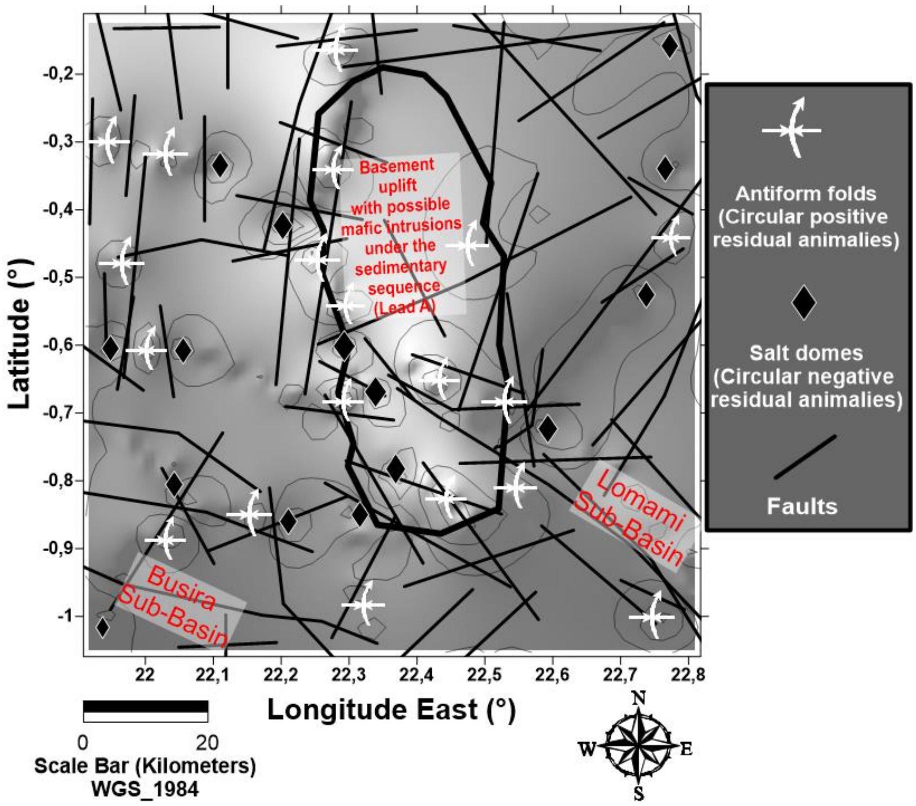

Fig. 15. Petroleum structural map of the region

The Congo Basin has undergone several tectonic events during its structural evolution. The Neoproterozoic rifting stage followed by the Pan-African (Neoproterozoic-Paleozoic) and Hercynian (Permo-Triassic) compressive events as well as the compression due to the opening of the East African Rift (Cenozoic-present) were therefore the basis of these multiple faults whose directions of major orientations in this zone are: NW-SE, N-S, E-W and NE-SW. The orientation in the N-S direction of the lead, the enormous faults which limit it as well as that of the antiform structures within it show us that the most important compression acted in the E-W direction in this region. These tectonic events also greatly favored the vertical movements of the Neoproterozoic salt layer and generated several salt domes clearly highlighted in this map. We also note that the uplift generated several listric inverse type faults on the lead.

These geological structures are of major oil interest: anticlines represent the most frequent and efficient type of oil trap with almost 80% of the world's recognized reserves. Faults can constitute barriers to the migration of hydrocarbons and traps called "fault traps", but they can also encourage the migration or dysmigration of hydrocarbons. Finally, thanks to the halokinesis phenomenon, salts play a very large role in the genesis of geological structures of major oil interest and their sides constitute barriers which hinder the movement of hydrocarbons on the surface and therefore promote their accumulation.

The correlated interpretation of the cross profile of gravity and magnetic anomalies calibrated with the R9 seismic profile allowed us to have a better image on the structural geology of this lead in order to better locate the oil targets (fig. 16).

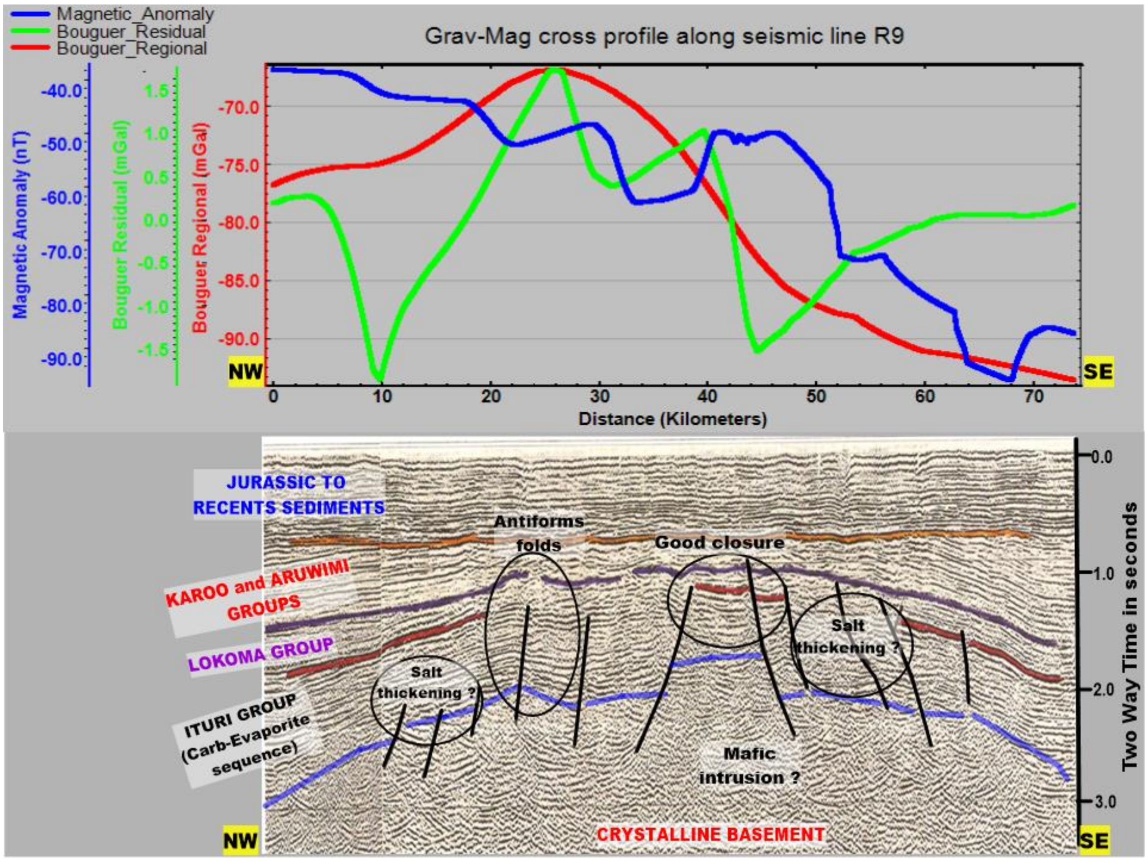

Fig. 16. Correlated interpretation of the gravity, magnetic and R9 seismic profiles

The regional bulge of the crystalline basement on the seismic profile is well represented on the curve of regional anomalies. The seismic profile also shows us that the top of the crystalline basement is very affected by faults which are certainly due to E-W compression followed by bulging. The multiple inflections of the magnetic anomalies curve would therefore be a response to these tectonic accidents which attack the basement. The high magnetic intensity (C1) located between 40 and 52 km probably represents a mafic uplift. The seismic profile also confirms that the sedimentary sequence from Jurassic to recent sediments is not affected by significant folding and breakage, unlike the entire sequence from the Lower Mesozoic-Paleozoic (Karoo and Aruwimi groups) to the Upper Neoproterozoic (Carbonate-Evaporite sequence from the Ituri group).

The large negative residual anomaly (B1) located 10 km away is the response to a probable thickening of the salt layer. The vertical succession of antiform folds encircled on the seismic profile correlates perfectly with the large positive residual anomaly (B2). These antiform folds are therefore priority oil targets. The half-width method told us that the depth of these structures would be around 2.5 km. The seismic profile tells us that the B3 anomaly represents the most important oil target. Indeed, this structure which is located in the center of the seismic profile could certainly be an area of strong accumulation of hydrocarbons: it is well limited to the east and to the west by two enormous faults which, at the same time, have certainly served as a migration drain for hydrocarbons from the underlying source rocks. On its top, the structure is limited by the Pan-African and Hercynian unconformities which act as closures in order to trap the hydrocarbons there. Its depth would be around 2.75 km.

The negative residual anomaly (B4) located between 40 and 50 km would also be due to the thickening of the salt layer. The seismic profile therefore confirms to us that the structural configuration of this zone could favor the retention of hydrocarbons on several levels.

7 Conclusion And Recommendations

This study concerns the detailed interpretation of the geophysical data acquired in block 7 of the Cuvette Centrale sedimentary basin in DR Congo in order to improve our knowledge of lead A. As a result, we have noticed that this structure is established on basement uplift wedged between the sub-basins of Busira in the west and Lomami in the east. It is therefore an ideal location to receive the oil expelled from these two depocenters. In addition, the multiple compressive events responsible for the establishment of this structural high also strongly affected the sedimentary sequence from the lower Mesozoic to the upper Neoproterozoic, causing the appearance of several folded, faulted structures and salt domes. These structures were clearly identified on the petroleum structural map drawn up at the end of this study and are of crucial importance both in the process of migration of hydrocarbons and in their trapping.

In order to increase the chances of discovery in this lead, we recommend that before carrying out a further seismic exploration and / or a first exploration drilling, the following studies be carried out:

- The reprocessing of the seismic lines R9, R10, R15, L53 and L54 which focus on lead A;
- The acquisition of surface oil indices near the Tshuapa river as well as a microbial geochemistry study on the entire extent of the lead.

Acknowledgments

We would like to thank the Société Nationale des Hydrocarbures du Congo (SONAHYDROC) for the geophysical data as well as the Faculty of Oil, Gas and New Energies of the University of Kinshasa and the Center of Research in Geophysics (CRG) for the software and laboratories.

References

[1] Marcio ROCHA MELLO (2006), Petroleum System Review of Busira and Lokoro Sub-Basins, Congo Central Basin, p. 13.
[2] Exploration Consultant Limited (ECL) (1988), Hydrocarbon potential of Cuvette Centrale, p. 39.
[3] COMIFAC (2005), Les forêts du bassin du Congo, Evaluation préliminaire.
[4] Bastien LINOL, Maarten J. De WIT, Erika BARTON, François GUILLOCHEAU, Michiel C.J. De WIT and Jean-Paul COLIN (2015), Paleogeography and Tectono-Stratigraphy of Carboniferous-Permian and Triassic 'Karoo-Like' Sequences of the Congo Basin, Geology and Resource Potential of the Congo Basin, Springer, p. 115.
[5] UNOCAL (1987), Reservoir Potential of samples from the Congo Basin, Zaire. International Report Unocal Science and Technology Division.
[6] ENI (2011), Cuvette Centrale Basin: Geological evolution and petroleum system analysis. Final Report, p. 12.
[7] Pierre EVRARD (1957), Les recherches géophysiques et géologiques et les travaux de sondage dans la Cuvette congolaise. L'académie royale des sciences coloniales.
[8] Jacques DUBOIS, Michel DIAMENT ET Jean-Pascal COGNE (2011), Géophysique: cours et exercices corrigés, 4ème édition, DUNOD, Paris, p. 9.
[9] Philip KEAREY, Michael BROOKS and Ian HILL (2002), An Introduction to Geophysical Exploration, 3rd edition, Blackwell Science, p. 137.
[10] Maroua ELFESSI (1996), Signatures gravimétriques de différents modèles géologiques.
[11] Michel CHOUTEAU (2002), Géophysique appliquée I: Magnétisme, Ecole polytechnique de Montréal, p. 32.
[12] Boualem BOUYAHIAOUI (2010), Etude de la croûte archéenne du môle In-Ouzzal (Hoggar Occidental) par la prospection gravimétrique: Identification des sources par la transformée en ondelettes, Université M'Hamed Bougara-Bourmerdes, p. 99.